Presented at the Materials Solutions Conference 2000 (October 10, 2000) St. Louis, MO

Diode Laser Cladding Produces High Quality Coatings

Authors:
1. Crystal M. Cook
2. John M. Haake
3. Mark S. Zediker

Conference: MATERIALS SOLUTIONS 2000

ABSTRACT

A high power direct diode [HPDDL] laser and its unique beam make for a highly efficient tool to use in cladding operations. Laser cladding is performed by melting a pre-placed powder onto a substrate to ensure a bond with minimal dilution, nominal melting and a small heat affected zone. The laser used in the experiment was the Nuvonyx ISL-4000L laser mounted on a Panasonic VR-16 robot. The pre-placed powders chosen for this experiment are ANVAL 410, 156 and C22. 410 and C22 were selected for their superior corrosion resistance. 156 is a general-purpose cobalt hardfacing material. The cladding substrate was ASTM 1018 steel. The dilution of the coatings was analyzed through the use of a Scanning Electron Microscope [SEM]. Through analysis it was discovered that dilution is kept to a minimum, in the range of 0 to .02%. The corrosion resistance and wear resistance was also measured for the appropriate samples. This

process is highly advantageous in comparison with competing coating methods such as plasma spraying, arc welding, and other laser sources. The rewards of the HPDDL are lower dilution and porosity, reduced post-machining, optimum edge detail.

1.0 INTRODUCTION

1.1 High Power Direct Diode Lasers As tools for use in industrial applications, HPDDL, also known as semiconductor lasers, are becoming more prevalent.[1,2,3] Diode laser technology has been used for a number of years in compact disks, laser printers and laser pointers. Their low cost, high efficiency (>55%), and compact design make them an attractive technology in the industrial manufacturing environment. The light emitted at the facet of the laser diode is highly divergent and astigmatic. To make this usable, a lenslet array is close coupled to a two dimensional array of laser diodes. Since the other axis, referred to as the "slow axis," is not collimated and is left to diverge, the final focusing lens will produce a concentrated line of light. This beam is very uniform, having a nearly tophat intensity profile along the long axis with a guassian profile perpendicular to the line along the short axis. The HPDDL used in this feasibility study employs 4 stacks of 20 bars, which are brought to a line by a single macro lens [Figure 1]. With dimensions of approximately 12.5 mm X <1 mm with a 125 mm focal length lens. With different macro lenses, this laser can achieve power densities greater than 200 kW/cm^2.

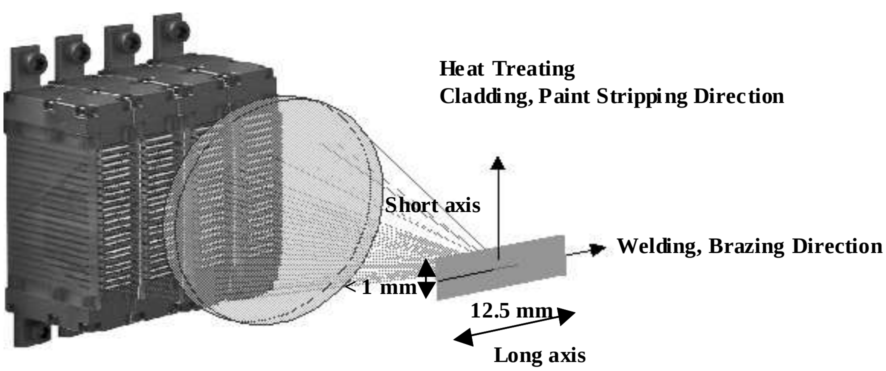

Figure 1 – Focus Configuration of Line Source HPLLD

An ideal application for the HPDDL is large surface area laser cladding. As shown in Figure 1, the line of laser light is moved perpendicular to the long axis along the short axis. The biggest benefit of HPDDL laser cladding is that the unique line source allows the user to produce clads with a controllable width without scanning. CO_2 and Nd: YAG lasers have a smaller spot; thus, the laser must be scanned over the cladded area. The wavelength of the HPDDL is 808 nm, compared with 1.06 μm for a Nd: YAG laser and 10.7 μm of the CO_2 laser. The shorter wavelength of the HPDDL allows for higher absorption into the material being cladded, therefore, a higher process speed can be achieved. Both CO_2 and Nd: YAG lasers often require binders when using pre-placed powders. The use of binders often leads to porosity due to the evaporation of volatiles during the cladding pass[4]. The HPDDL system does not necessitate the use of binders to hold the powder together before a cladding pass. Another advantage of the HPDDL is a solid state laser; thus, the thermal input can be precisely controlled, yielding minimal dilution and a small heat affected zone.

1.2 Laser Cladding During a laser cladding process, dilution is expected to be minimized. In cladding operations dilution, is often defined as the amount of intermixing of the clad and substrate with current cladding techniques. Dilution is measured by visual analysis or through a SEM elemental line scan. Visual analysis allows the user to get a quick estimate of the dilution of the clad, however, with the HPDDL this method of measurement was found not to be very accurate. Through visual analysis, dilution is defined as the distance the clad layer extends below the substrate. SEM analysis is a true, accurate measure of the dilution, or intermixing of the clad and substrate. Laser alloying is a process that is often grouped with laser cladding operations. Laser cladding and alloying are traditionally distinguished by the relative amounts of the consumable material added and substrate melted. Generally the two categories are arbitrarily separated by their relative amount of dilution, laser alloying being classified as having greater than 10% dilution, laser cladding having less than 10% dilution[4]. In laser alloying it is generally desired to mix portions of the coating with the substrate to produce an alloyed layer, thus a high dilution and high intermixing is expected. It should also be noted that laser alloying requires convection in the weld pool and laser cladding does not. In many laser alloying processes, the cooling rate is often monitored to ensure intermixing and the formation of unique metallurgical compounds. Ultrafast quench rates of the order of 10^{11} Ks^{-1} are often required[4] as well as a high solubility of the clad material in the parent material. Laser alloying experiments were not conducted in this study; however, throughout the experimentation there was an expectation that at a low process speed some alloying of the powder and substrate may occur. This was not true for the HPDDL process which has low quench rates and a non-turbulent melt pool unlike Nd:YAG and CO_2 lasers.

The clad material deposited with the HPDDL does not intermix with the substrate in many applications; therefore, the dense, uniform microstructure of the clad layer allows for enhanced single pass corrosion or wear resistance. The denser microstructure and better bonding of laser clads allows for enhanced corrosion and wear resistance with a single pass. Laser cladding is a viable alternative to plasma spraying and TIG or MIG processes. It is difficult to produce a clad with a TIG, MIG or plasma spray system without having less than 5% dilution, therefore, as many as 15 overlapping passes may be required to obtain an undiluted clad layer[5]. Conventional arc welding processes generally impart a significant amount of heat into the part resulting in a large heat affected zone and distortion. Post-weld treatment can improve the properties of the joint, but can also lead to distortion of the component[6]. The surface finish of overlapping passes produced with the HPDDL are relatively flat, however, a TIG cladding process often results in distinct ridges and valleys, which lead to cracking when bent[7]. In addition, the arc welding processes often are also responsible for the losses of alloying elements[8]. A direct comparison of a laser clad layer with an arc-welded layer indicates that the HPDDL clad has significant grain refinement, which in some cases lead to an increased wear resistance[9]. Laser cladding also has advantages over plasma clad processes. The sharp intermetallic boundary of the plasma clad layer with the substrate also often leads to pores and cracking[9]. The interface between the clad and substrate of a HPDDL clad is smooth with minimal dilution and no boundary layer. The HPDDL also surpasses flame spray technology, since flame spray produces a more porous coating with limited adhesion[10].

2.0 **MATERIALS SELECTION**

The properties of the clad material alone will not determine the properties of the clad on the substrate. The solubility of the clad, which determines the amount of intermixing of the clad and substrate, i.e. dilution, is important. The resulting microstructure of the clad, the dilution layer and heat-affected zone are all important areas in determining the quality of the clad. Solubility and wetting issues that lead to pits and pores also affect the quality of the clad. All of the above influence the wear and corrosion resistance of the clad.

Wear and corrosion resistant powders were selected for the experimentation. The corrosion resistant powders include C22, which is a NiCrMo alloy in the Hastealloy C family, and 410, which is a basic stainless T410 material. The nominal composition of each alloy is listed in Table 2. The substrate used was 1018 steel, which was selected because it is a commonly used and is an inexpensive material. The 156 material is a cobalt based hardfacing alloy used for increased wear resistance. The composition of this alloy consists mainly of cobalt, however Cr is also largely alloyed in this material [Table

Material	UNS	SS	C	Cr	Ni	W	Fe	Co	V	Mo
410	***S 41000***	2302	0.1	12.5	--	--	--	--	--	--
156	***Stellite 156***	--	1.1	28.0	<3.0	1.0	< 0.5	Bal	--	--
C22	***--***	--	<.02	21.5	Bal	3.0	5.0	--	0.15	13.5

1].

Table 1: Nominal compositions of the clad materials.

3.0 EXPERIMENTAL

3.1. Experimental Procedure The powder was pre-placed to a thickness of .050" on a 1018 steel substrate. The line source was passed along the short axis over the powder. The speeds varied from 0.3 to 0.8 m/min at 4 kW of laser power. The variance in the speed allowed for clads to be produced with varying levels of visual dilution. Each powder was cladded with a visual dilution of 0%, 10% and 60%. The thickness and width of the cladding pass changes with modifications in processing speed. As the processing speed increases the clad track has an increasingly gaussian profile due to the surface tension of the melt. However, a decrease in speed results in a flatter, wider clad with high visual dilution [Figure 2]. Overlapping passes wet together to form a relatively flat

profile regardless of processing speed.

Figure 2: A comparison of the profiles of three NiCrMo clads. The clad in the middle was produced at a travel speed of 0.45 m/min, the clad to the left at a process speed of 0.70 m/min. The clad to the right is an overlapping pass sample.

All of the clads were sent for SEM analysis, one of the hardfacing clads at each dilution level was sent for wear testing and the corrosion resistant clads were used for corrosion analysis. SEM analysis was completed to determine the level of dilution and change in dilution with overlapping passes. The profile of these samples was a relatively flat surface. Corrosion testing was done on the stainless steel samples by immersing the samples in a 75°C bath of 20% nitric acid for a period of 40 hours. The NiCrMo clads were also tested by immersion into a 80% phosphoric acid bath for 40 hours. Wear testing was done on the Cobalt based clad layer. The standard pin on disk test was done in accordance with ASTM G99 to determine the resistance to galling of the clad.

3.2 Standard Visual Examination After the clads were produced with the HPDDL a portion of each clad was cut off, ground with 180 grit paper, and etched in 2% Nital to determine the visual dilution. The portion of the clad that was above the substrate was measured at the highest point as well as the entire length of the clad layer. The portion of the clad below the substrate was divided by the length of the total clad layer to produce a percentage visual dilution [Figure 3]. The initial dilution measurements described above are shown in Table 2. The drawback to this method of measuring dilution is the lack of accuracy in measurements, due to the fact that the amount of alloying cannot be determined with this method. However, visual dilution measurements are a straightforward approach to determining the approximate dilution of a sample while processing.

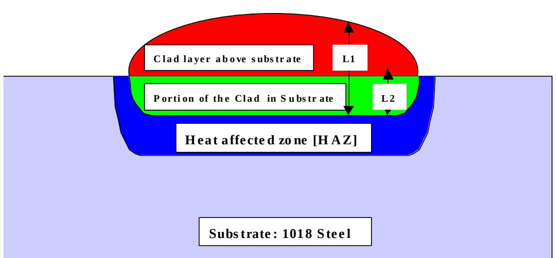

Powder	Speed (m/min)	Power (kW)	Dilution (%)
Stainless Steel	0.30	4.0	29
Stainless Steel	0.65	4.0	10
Stainless Steel	0.70	4.0	0
Cobalt Based	0.40	4.0	40
Cobalt Based	0.70	4.0	20
Cobalt Based	0.75	4.0	0
NiCrMo	0.45	4.0	40
NiCrMo	0.70	4.0	17
NiCrMo	0.80	4.0	0

Figure 3: Standard visual measurement of dilution was performed through the equation L2/L1.

3.3 Microstructural Characterization To bring out the microstructure, the 410T stainless material was electrolytically etched in oxalic acid, while the NiCrMo and cobalt based alloys were etched electrolytically in a solution containing equal amounts of CrO_3 and potassium permanganate, and 8% sodium hydroxide. The microstructures indicate thorough melting of the powder. Both the NiCrMo and Cobalt based alloy show a dendritic microstructure within the clad layer [Figure 4]. Grain growth is seen in the heat affected zone of the clad, however, there is no evidence of the melting of the substrate. The 410 T SS powder shows also shows grain growth in the heat affected zone, but the microstructure of the clad show is primarily martensitic due to the rapid quench rate of the powder. The microstructures present indicate that the dilution of the clad into the substrate is minimal and that changes in process speed do not reflect changes in dilution.

Figure 4: Dendritic formation in the Cobalt based clad layer, also the interface between the clad and substrate is shown on the left.

3.4 SEM Analysis A SEM elemental trace was used on each of the samples to determine the dilution of the clad layer as defined by the amount of intermixing of the clad layer and substrate. Each powder has a reasonable amount of Chromium; therefore, this element was traced in the clad layer for each powder. Iron was traced in the substrate.

At both a low and high process speed the dilution of the clad into the substrate is minimized. This can be seen in Figures 5, 6 and 7. The NiCrMo powder was clad at a speed of 0.45 and 0.7 m/min at a power of 4 kW.

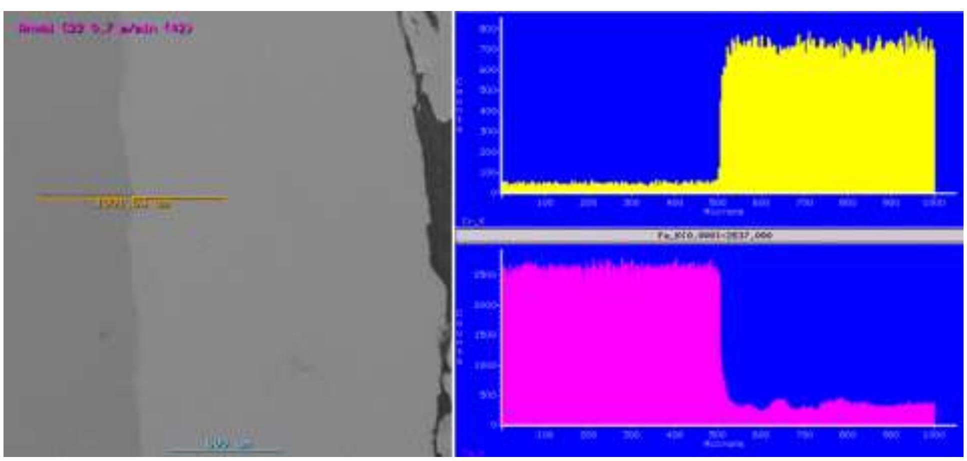

Figure 5: NiCrMo alloy clad at 0.7 m/min, 4 kW.

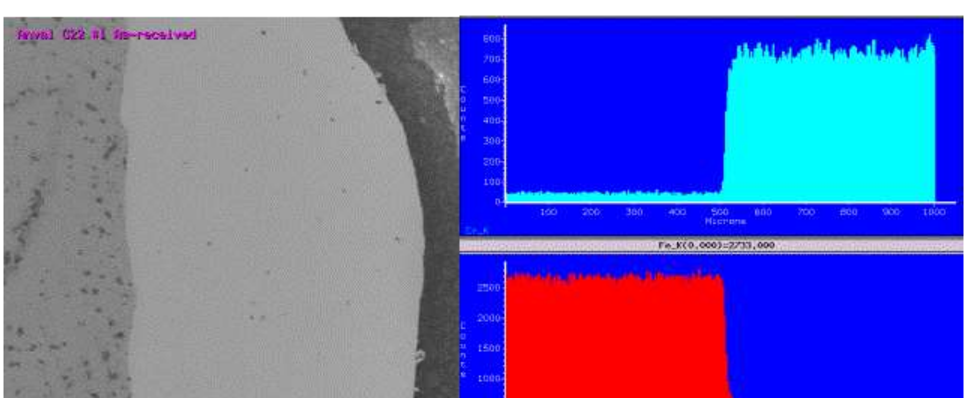

Figure 6: A SEM line trace of a NiCrMo clad produced at 0.45 m/min, 4 kW.

The properties of overlapping passes with regard to dilution and amount of intermixing are similar to those of a single pass. The same NiCrMo based powder has minimal dilution and intermixing at a process speed of 0.7 m/min, 4 kW [Figure 7].

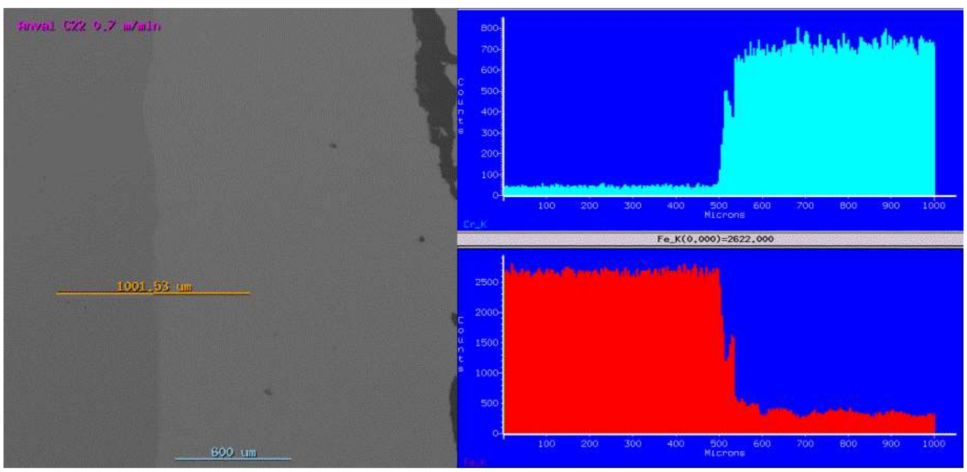

Figure 7: SEM line trace of overlapping passes of NiCrMo alloy produced at 0.7 m/min, 4 kW.

Samples produced with the cobalt based and stainless steel powders produced similar results with respect to dilution. Dilution was minimal at all of the process speeds. As overlapping passes are produced to create a 100% clad surface, no effect on dilution is observed.

3.5 Corrosion Testing Corrosion testing was performed on the stainless steel samples by immersing the clad and substrate in a solution of 20% nitric acid, 80 % de-ionized water at 75°C for a period of forty hours to determine the effect acid on the clad. Corrosion testing was also completed on the NiCrMo alloy by immersing the clad in a 80% phosphoric acid, 20% de-ionized water solution at 120°C for forty hours. The mass of each sample was recorded every four hours; the oxide was removed from each sample before they were weighed. The corrosion rate for each sample was calculated through the equation:

Corrosion Rate = (K*W)/(A*T*D)

Where: K = 3.45*(10^6) mils/year

T = time of exposure in hours to the nearest 0.01 hour

A = area in cm^2 to the nearest 0.01 cm^2

W = weight loss in g, to the nearest 1 mg

D = density in g/cm^3

Figure 8 shows the change in mass for each sample and the corrosion rate for each sample of 410 stainless steel. Both oxidized and unoxidized samples were tested to determine the effect of oxidation on the corrosion resistance of the samples. It was found that the oxidized samples had a slightly lower corrosion rate than the oxidized samples. The average corrosion rate for the oxidized samples was 15 mils/year, the average corrosion rate for the unoxidized samples is 30 mils/year. No conclusions can be drawn on the effect of process speed on the corrosion resistance of the samples.

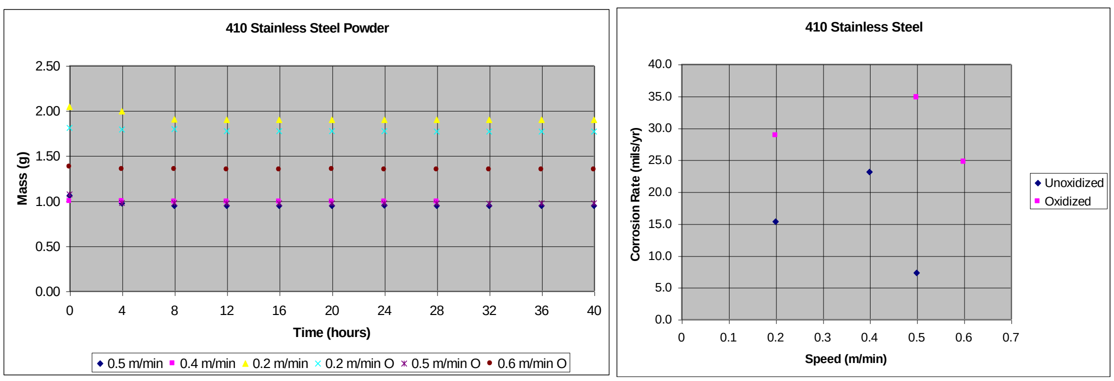

Figure 8: Mass loss and corrosion rate data for the 410 stainless steel samples.

A region of corrosion instability on the iso-corrosion diagram [Figure 9] was chosen for the NiCrMo clads. All of the samples were un-oxidized, the process speed varied from 0.45 to 0.70 m/min.

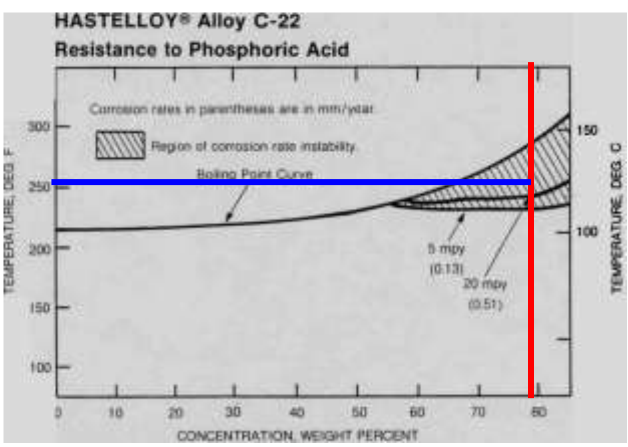

Figure 9: Iso-corrosion diagram for the C22 alloy as well as the mass loss for each sample.

3.6 Wear Testing

3.6.1 Pin on Disk To produce consistent values for relative wear resistance, a standard pin-on-disk wear testing machine was used in accordance to ASTM standard G99. The data indicates that with a slower processing speed the wear resistance will slightly increase, or the percent mass loss will decrease [Figure 10]. The 0.40 m/min observed a slightly lower mass loss than that of the samples produced at faster speeds. The decrease in mass loss with a decrease in speed is due, in part, to the denser microstructure produced at a slower speed. The overlapping passes also have a slightly lower loss of material than the single pass samples. The decrease in mass loss is not significant enough to draw reasonable conclusions. However, this may be a slight indication that the overlapping passes have superior properties than single pass samples due to increased surface roughness and the denser microstructure. It is also visible from figure 11 that the mass loss of all of the clad layers is significantly less than that of the substrate.

Sample	Revolutions	% Cumulative Mass Loss
0.40 m/min, 4 kW	1000	0.26
0.40 m/min, 4 kW	2000	0.42
0.40 m/min, 4 kW	3000	0.56
0.40 m/min, 4 kW	4000	0.68
0.40 m/min, 4 kW	5000	0.79
0.70 m/min, 4 kW	1000	0.13
0.70 m/min, 4 kW	2000	0.35
0.70 m/min, 4 kW	3000	0.54
0.70 m/min, 4 kW	4000	0.69
0.70 m/min, 4 kW	5000	0.81
0.75 m/min, 4 kW	1000	0.39
0.75 m/min, 4 kW	2000	0.55
0.75 m/min, 4 kW	3000	0.73
0.75 m/min, 4 kW	4000	0.93
0.75 m/min, 4 kW	5000	1.12
Overlapping Passes, 0.70 m/min, 4 kW	1000	0.26
Overlapping Passes, 0.70 m/min, 4 kW	2000	0.31
Overlapping Passes, 0.70 m/min, 4 kW	3000	0.39
Overlapping Passes, 0.70 m/min, 4 kW	4000	0.46
Overlapping Passes, 0.70 m/min, 4 kW	5000	0.56
Substrate: 1018 Steel	1000	0.55
Substrate: 1018 Steel	2000	1.08
Substrate: 1018 Steel	3000	1.59
Substrate: 1018 Steel	4000	2.09
Substrate: 1018 Steel	5000	2.60

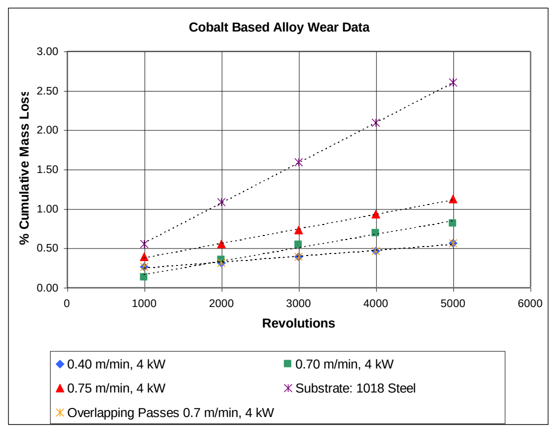

Figure 10: Pin on Disk wear test results.

4.0 CONCLUSIONS

Through experimentation it was found that the HPDDL is an effective method of producing high quality clads with minimal dilution. It was found that the corrosion and wear properties of HPDDL clads are equal to those produced with competing methods such as plasma spray, TIG or MIG deposits. The HPDDL allows the user to produce a single pass clad with minimal dilution. This cannot be accomplished by traditional arc welding processes, which require multiple passes to achieve a pure clad layer. The low dilution clads with controllable thickness are beneficial because the end user can save the expense of purchasing excessive amounts of cladding wire and powder. Laser cladding is highly advantageous over TIG and MIG processes because the amount of dilution is controllable, it is an automated process, chemically clean and environmentally friendly. The primary advantage of the HPDDL in comparison to CO_2 and Nd:YAG lasers is the shorter wavelength and thus higher absorption of the direct diode laser. Other benefits of the HPDDL over conventional lasers are the elimination of scanning, controllable dilution and the elimination of binders with pre-placed powders. The HPDDL is a highly capable cladding tool that will produce coatings with first-rate corrosion and wear resistance, low dilution, low porosity, unique microstructures and aesthetic surface finishes.

5.0 REFERENCES

1. P. Loosen et. al., SPIE, 2382 , 78-87 (1987).
2. S. Pflueger et. al. "Material Processing with high Power diode lasers", Automotive Laser Applications. 1995 workshop.
3. S. Pflueger and F. Kuepper, ESD Technology, April/May 1996.
4. S. V. Joshi and G. Sundararajan in N. Dahotre, ed. Lasers in Surface Engineering, ASM International, Ontario, 1998, pp.121-124, 139-144, 149-153.
5. C. L. Horn et. al. in T. Lyman. Metals Handbook: Welding and Brazing, American Society for Metals, Metals Park, 1981, pp. 149-161.
6. K. C. Meinert, Jr. and P. Bergan, ICALEO 1999 Proceedings, 87, F49 (1999).
7. T. Heston, Welding Journal, 79 (7), 46 (2000).
8. H. Ocken, Advanced Materials and Processes, 157 (6), 103 (2000).
9. B. Medres, L. Shepeleva and M. Bamberger in ref. 6, pp. F225-F230.
10. R. Hull et. al. in ref. 6, pp. 41,45-47.
11. ASTM Standard G31-72 (1999) ASTM Subcommittee G01.05.